

Geothermal power plant case study for a new ORC plant including CO₂ reinjection

Daniele Fiaschi^{1*}, Vitantonio Colucci², Giampaolo Manfrida³, Lorenzo Talluri⁴.

¹⁻⁴University of Florence, Department of Industrial Engineering, Viale Morgagni 40-44, 50134, Florence

*corresponding author: daniele.fiaschi@unifi.it

Keywords: geothermal power, total reinjection, ORC, CO₂.

ABSTRACT

A closed-loop ORC power plant layout including complete gas reinjection for the geothermal location of Castelnuovo Val di Cecina, Italy is proposed and analysed. The reservoir conditions correspond to a live steam field, with relevant contents of CO₂ and acid gases in the resource. The proposed solution includes complete reinjection of the non-condensable gases, using an intercooled compressor train to reinject the gas at suitable depth within the condensate stream. A sub-critical single-pressure ORC using R245fa or R1233zd(E) is taken as the reference case and optimized conditions for efficiency and power are determined. The effect of the CO₂ content in the resource is investigated and discussed. The calculations include the piecewise solution of the main heat exchanger; a detailed exergy balance and exergo-economic analysis is done, allowing the evaluation of the final cost of electricity, and the contributions to this last of capital costs and of irreversibilities in the process.

1. INTRODUCTION

The commitments made by European Union countries on the reduction of energy produced by fossil fuels up to 2030 through the agreements signed in the three COPs of Paris (December 2015), Marrakech (November 2016) and Katowice (December 2018) will contribute to the containment global warming and beneficial effects on energy saving. Within this scenario, geothermal energy represents a clean resource, which is positioned to play an important role in mitigating global climate change, fostering a reduction of greenhouse and other gas emissions by replacing fossil fuels for power generation (Afgan, N.H. and Carvalho, M.G., 2002). Therefore, the role of geothermal energy in the forthcoming decades is of fundamental importance for guaranteeing clean energy consumption in compliance with the commitments made on decarbonisation undertaken at international level: overall containment within agreed limits (max + 2 °C compared to pre-industrial values period).

Geothermal power plants emit very limited amounts of pollutants (mainly H₂S, NH₃ and in some cases Hg), with available solutions for emissions treatment; a wide scatter among different plants and sites is documented in terms of greenhouse emissions (from 100 to over 800 g/kWh, compared to 375-1000 g/kWh for fossil-fuel power plants). However, it is questionable whether these greenhouse emissions would anyway – at least partially – reach the surface, and substitution of fossil-fuel electricity production with geothermal is anyhow positive (Di Pippo, 2007; Bertani and Thain, 2002; Manfrida et al. 2016; Kasameyer, 1997). Sustainable development of geothermal resources requires methods and tools to control their environmental impacts (Eylem K. et al. 2018). Several countries, such as Italy, which has an over-100yr tradition in using the geothermal resource, are making substantial efforts to bring down emissions levels. Geothermal energy plays relevant roles in Europe for the production of electricity and for direct applications.

In recent years, the traditional schemes for geothermal energy conversion (based on direct use of steam or flashing high-pressure water resources) have been put in discussion, first in the low/medium temperature applications ($T_{GR} = 100-140^{\circ}$). The new technology for power generation applies the binary cycle concept, that is, an organic Rankine cycle (ORC). This solution avoids the direct use of the geothermal fluid as cycle working fluid, and becomes particularly attractive when complete reinjection of the resource (brine+non-condensable gas NCG) is considered. The operating principle of a binary/ORC cycle is to extract the heat from the geothermal fluid through a heat exchanger and transfer it to a low-boiling-point organic fluid or mixture. The working fluid evaporates and is expanded into a turbine and recovered through a cooled condenser in closed cycle. Heat extraction from the geothermal fluids can be maximized through efficient heat exchangers and by the selection of appropriate working fluids (Vaccaro et al., 2016). Hydrocarbons have played an important role in demonstrating feasibility of ORC technology; today, special fluids such as Siloxanes, R245fa and R1233zd(E) can be proposed for geothermal resources below $T_{GR} = 250^{\circ}C$. They are non-corrosive, substantially non-flammable

and non-reactive at the operating or ambient pressure and temperature.

Reinjection of the resource is practiced since 1980 in geothermal fields for the condensed liquid of direct steam or flash power plants (Di Pippo, 2007). On the other hand, the geothermal fluid contains non-condensable gas (NCG) such as CO₂, which is the most common gas, typically ~ 90% of the total NCG; plus contaminants, mostly H₂S; the NCGs, are usually not reinjected but extracted from the condensers and vented to the atmosphere (in Italy, H₂S, Hg and NH₃ are efficiently removed before that by chemical treatment). Currently, important demonstration projects (CARBFIX, Wairakei; ContactEnergy, 2010) are proving feasibility of NCG reinjection, and this technology is making quick steps thanks to knowledge advancements in other fields (such as oil and gas, and CCS). Reinjection of NCGs could cause problems, such as groundwater contamination and leakage of reinjected fluid to the surface, which must be evaluated by accurate geological studies of the local context. In practice, reinjection of NCGs has been applied to the geothermal sector in few fields and countries (Ingimundarson, 2015; CARBFIX, 2019). The injected CO₂ can be in the form of gas, supercritical fluid or dissolved in brine. Injection of CO₂ together with brine is usually preferred to single-phase CO₂ injection. The injection of dissolved CO₂ into geothermal reservoirs leads to several advantages compared to supercritical CO₂ sequestration in CCS applications. A mixture of brine-CO₂ improves residual entrapment, prevents geo-mechanical damage due to overpressure and avoids the risk of gas escaping from the reservoir. Although challenging from the technical point of view, the reinjection of CO₂ can be useful in the production of steam because the presence of CO₂ in the fluid preserves the pressure of the flash point of the fluid mixture, promotes boiling and enhances the enthalpy of the fluid produced by the reservoir (Kaya and Zarrouk, 2017).

2. METHODOLOGY

2.1 Modelling of CO₂ and H₂O mixtures (Geothermal fluid)

Most optimization studies for geothermal power plants are performed assuming that the geothermal fluid is pure water. In the present case, the resource (Castelnuovo Val di Cecina site, Italy) is in saturated steam conditions with an expected NCG mass content of about 8%. While transferring heat to the binary/ORC circuit, the steam is condensed and most of the gas phase is composed of CO₂, which must be compressed and reinjected at a suitable depth in the reinjection well. Thus, it is necessary to be able to treat the complete water/steam two-phase region including CO₂ dissolved in the liquid; the gas mixture is mainly composed of CO₂, but initially there is a non-negligible steam fraction. For the present case, the fluid is in general a mixture of water and CO₂: the temperature range extends from 10 °C to 260 °C, while the production

wellhead pressure is about 1000 kPa. The geothermal fluid chemistry, density and boiling-depth relationships are controlled, to some extent, by the concentration of carbon dioxide (Mahon et al., 1980b). A reservoir fluid with > 2% CO₂ in mass experiences the H₂O phase transition at larger depth than a low-gas geothermal fluid having the same temperature. The effect of the gas on the depth at which boiling first occurs is the greatest in the range 150-200 °C, where the solubility of carbon dioxide into the liquid phase shows a minimum.

The partial pressure of carbon dioxide decreases with increasing temperature (Arnorsson et al., 1982) for carbon dioxide composition beyond 2% in mass in a H₂O-CO₂ mixture. Figure 1 shows the partial pressure of CO₂ as a function of temperature at 1000 kPa.

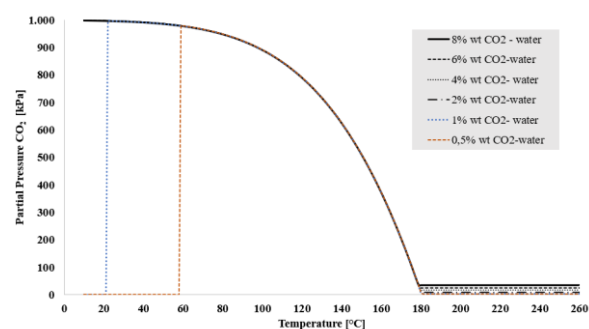


Figure 1: Partial pressure of carbon dioxide of a geothermal fluid from 0.5% wt. to 8% wt. CO₂ versus temperature at 1000 kPa total pressure.

In order to evaluate the potential of water as carbon dioxide absorber, the solubility of CO₂ in water at different temperatures and pressures was investigated by different Authors (Kohl and Nielsen, 1997; Duan and Sun, 2003). All models agree that the CO₂ solubility decreases with increasing temperature, certainly up to a pressure of about 10 MPa.

Considering that the pressure conditions for the Castelnuovo Val di Cecina site are moderate (1000 kPa at production wellhead) with respect to the critical pressures of both fluids, it was considered sufficient to approach the CO₂-H₂O mixture properties with a third-order EOS model. This choice also derives from the fact that the thermodynamic model solves the system with high efficiency and reliability, with very reduced calculation time.

The property package was implemented in Unisim Design (Unisim, 2018); Peng-Robinson (PR) or Soave-Redlich-Kwong (SRK) EOS were considered. The VLE and the enthalpy/entropy are calculated by means of the EOS. The Peng-Robinson EOS supports the widest range of operating conditions and the largest variety of systems; it is convenient for geothermal fluids as it allows to incorporate experimentally-tuned coefficients for the interaction parameters of CO₂ and H₂O. The following Table 1 provides a list of the

equations used in UniSim Design for the PR EOS modelling the geothermal fluid.

	$P = \frac{RT}{V-b} - \frac{a}{V(V+b) + b(V-b)}$ $Z^3 - (1-B)Z^2 + (A-2B-3B^2)Z - (AB-B^2-B^3) = 0$
where:	
$b=$	$\sum_{i=1}^N x_i b_i$
$b_i=$	$0,077796 \frac{RT_{ci}}{P_{ci}}$
$a=$	$\sum_{i=1}^N \sum_{j=1}^N x_i x_j (a_i a_j)^{0,5} (1 - k_{ij})$
$a_i=$	$a_{ci} \alpha_i$
$a_{ci}=$	$0,457235 \frac{(RT_{ci})^2}{P_{ci}}$
$\alpha_i^{0,5}$	$1 + m_i (1 - T_{ri}^{0,5})$
$m_i=$	$0,37464 + 1,54225\omega_i - 0,26992\omega_i^2$ <p>if $\omega_i > 0,49$</p> <p>else $0,379642 + (1,48503 - (0,164423 - 0,016666\omega_i)\omega_i)\omega_i$</p>
$A=$	$\frac{aP}{(RT)^2}$
$B=$	$\frac{bP}{RT}$

Table 1: Equations used in geothermal fluid modelling with Unisim Design (PR EOS)

For the purpose of this application, which deals with a mixture condensing H₂O at a fixed pressure of 1000 kPa, the results of the simulation of the H₂O-CO₂ geothermal fluid for various % wt. CO₂ are best shown in terms of the temperature glide during the condensation process on T-s diagram (Figure 2). Pure water data from steam IAPWS formulation are also plotted for comparison.

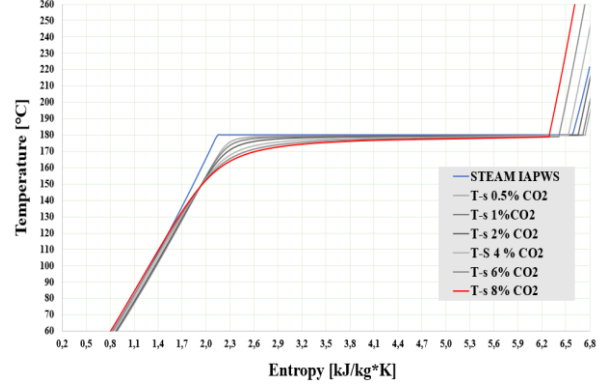


Figure 2: T-s diagram of water- CO₂ mixture

2.2 ORC and intercooled compressor train modelling

The design ORC configuration for the Castelnuovo Val di Cecina site is shown in Figure 2. The ORC scheme is recuperative, basically composed of a pump, a turbine, a condenser, an evaporator and a recuperator. The model of the whole power plant was developed in EES programming environment (Nellis, Klein, 2019), taking advantage of the thermodynamic properties package, available for different working fluids. The properties of the water-CO₂ mixture of (geothermal resource) were imported from the Unisim model, using lookup tables to transfer the data to the ORC simulation code.

The power plant calculations were performed assuming steady state processes, adiabatic behaviour of pumps, turbines and compressor and dead state conditions of 298 K and 101 kPa.

Mass and energy balances were applied to all components, as resumed in Eqns. [1] and [2].

$$\sum \dot{m}_i = \sum \dot{m}_e \quad [1]$$

$$\sum \dot{Q} + \sum \dot{m}_i h_i = \sum \dot{W} + \sum \dot{m}_e h_e \quad [2]$$

where \dot{Q} and \dot{W} stand for heat and work transfers across the component boundaries; \dot{m} and h are respectively the mass flow rate and the specific enthalpy of each stream.

The net produced power by the ORC cycle takes into account not only the consumption of the pump, but also that of the compressor train, as shown in Eq. [3]:

$$\dot{W}_{net} = \dot{W}_t - \dot{W}_p - \dot{W}_c \quad [3]$$

The net power output is fixed at 5 MW, as the selected case study (Castelnuovo Val di Cecina) falls into the regulatory guidelines limit for a pilot power plant with high NCG content. The resource conditions at power plant inlet is saturated vapour at 180°C, 1000 kPa and 8% CO₂ in mass (Vaccaro et al., 2016).

The geothermal resource is cooled in the main heat exchanger and water condensation takes place. At the present stage of the model, the solubility of CO₂ in water is neglected; consequently, the stream 31 is assumed as pure water and stream 40 is pure CO₂. Therefore, this assumption considers the worst-case scenario for total reinjection, as the whole mass flow rate of CO₂ entering the power plant needs to be compressed to allow the total reinjection.

In order to reduce the required power of the compressors train, one precooler and two intercoolers are considered. The heat exchanged in these components can be recovered and utilized for a small district heating network. In the present study, the inlet temperatures of the pre cooler and intercoolers network (point 50, 52, 54) were assumed at 20°C and a minimum 10°C ΔT was considered for these heat exchangers.

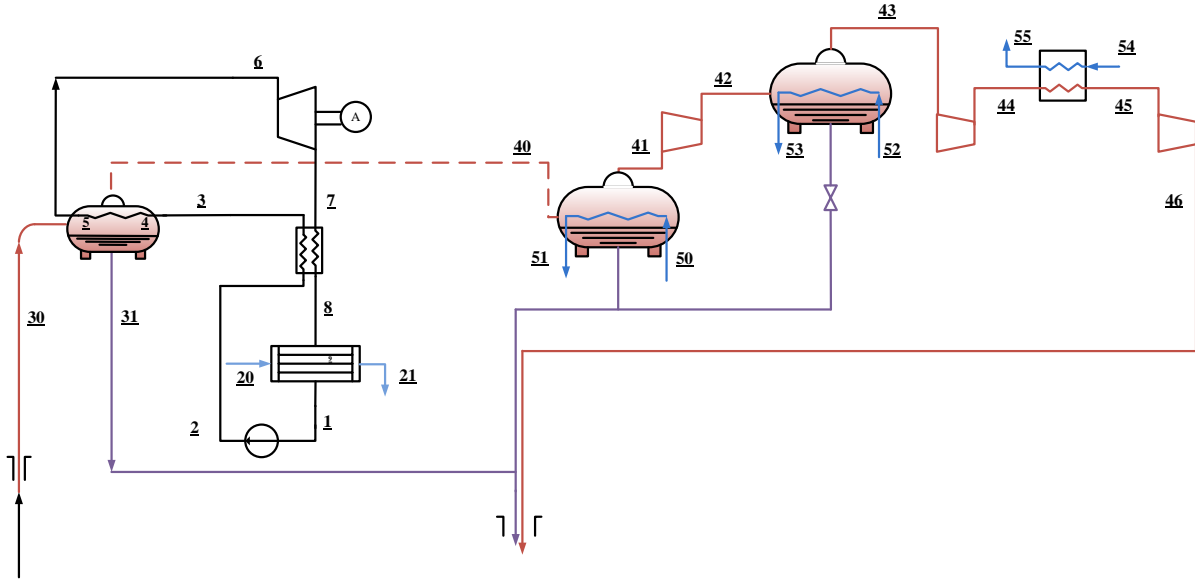


Figure 3: Power plant schematic.

2.3 Exergy and exergo-economic analyses

An exergy analysis (Kotas, 1985; Szargut et al., 1988) was applied to estimate the source of inefficiencies of the system components, as it combines both first and second principle of thermodynamics. Exergy balances were applied to calculate the exergy destructions (Bejan et al., 1995) and losses to the environment from each plant component, as shown in Eq. [4]:

$$\dot{E}x_{di} + \dot{E}x_{li} = \sum \dot{m}_i ex_i - \sum \dot{m}_e ex_e + \dot{E}x_Q + \dot{E}x_W \quad [4]$$

Where $\dot{E}x_d$ and $\dot{E}x_l$ represent respectively the exergy destruction and loss rate of the generic component i , $\dot{E}x_Q$ and $\dot{E}x_W$ (positive if produced by the component) are the exergy rates due to work and heat transfer and $\dot{m} \cdot ex$ represents the flow exergy rate carried with the in/out streams through the system. The exergy destructions represent the irreversibility introduced by the components; while exergy losses represent the exergy directly lost to the environment.

An exergo-economic analysis (Bejan et al., 1995) was applied to determine the economic profitability of a power plant, taking into account the useful fraction of energy only (exergy). The exergo-economic analysis also shows the progressive build-up of costs of the different streams flowing through the powerplant components, thus it is very useful to decide which components could more profit to invest in for improvement, in order to enhance the overall thermoeconomic performance of the power station.

The exergo-economic balances are evaluated considering the contribution of the investment and maintenance costs, as shown in Eq. [5]:

$$\sum_{\text{output}} \dot{C}_{P,\text{tot}} = \sum_{\text{input}} \dot{C}_{F,\text{tot}} + \dot{Z}_{\text{tot}}^{CI} + \dot{Z}_{\text{tot}}^{OM} \quad [5]$$

$\dot{Z}_{\text{tot}}^{CI}$ and $\dot{Z}_{\text{tot}}^{OM}$ are computed dividing the total annual investments, operation and maintenance costs, by the total yearly working time. The calculation of the components cost was carried out following the methodology proposed in Turton et al., 2009. The obtained values were discounted to the reference year (2019) through the CEPCI (Chemical Engineering Plant Cost Index) inflation index.

Table 2 resumes the exergo-economic balances and the required auxiliary equations (Bejan et al., 1995), which are required to solve the cost equations applied to each component.

Table 2 –Thermo-economic balance equations of powerplants components

Component	Exergo-economic balances
Pump	$c_2 \cdot \dot{E}xt_2 = c_1 \cdot \dot{E}xt_1 + c_{Wp} \cdot \dot{W}_p + \dot{Z}_1$ $c_{Wp} = c_{Wt}$
HE	$c_8 \cdot \dot{E}xt_8 + c_3 \cdot \dot{E}xt_3 = c_7 \cdot \dot{E}xt_7 + c_2 \cdot \dot{E}xt_2 + \dot{Z}_2$ $c_8 = c_7$
HE_{Geo}	$c_6 \cdot \dot{E}xt_6 = c_3 \cdot \dot{E}xt_3 + C_{Geo} + \dot{Z}_3$ $C_{Geo} = c_{fuel} \cdot (\dot{E}xt_{30} - \dot{E}xt_{31} - \dot{E}xt_{46})$
Turbine	$c_{Wt} \cdot \dot{W}_{turbine} + c_7 \cdot \dot{E}xt_7 = c_6 \cdot \dot{E}xt_6 + \dot{Z}_4$ $c_7 = c_6$
Condenser	$c_1 \cdot \dot{E}xt_1 = c_8 \cdot \dot{E}xt_8 + \dot{Z}_5$
Pre cooler	$c_{41} \cdot \dot{E}xt_{41} = c_{40} \cdot \dot{E}xt_{40} + \dot{Z}_6$ $c_{40} = c_{fuel}$
C1	$c_{42} \cdot \dot{E}xt_{42} = c_{41} \cdot \dot{E}xt_{41} + c_{Wc1} \cdot W_{c1} + \dot{Z}_7$ $c_{Wc1} = c_{Wt}$
IC1	$c_{43} \cdot \dot{E}xt_{43} = c_{42} \cdot \dot{E}xt_{42} + \dot{Z}_8$
C2	$c_{44} \cdot \dot{E}xt_{44} = c_{43} \cdot \dot{E}xt_{43} + c_{Wc2} \cdot W_{c2} + \dot{Z}_9$ $c_{Wc2} = c_{Wt}$
IC2	$c_{45} \cdot \dot{E}xt_{45} = c_{44} \cdot \dot{E}xt_{44} + \dot{Z}_{10}$
C3	$c_{46} \cdot \dot{E}xt_{46} = c_{45} \cdot \dot{E}xt_{45} + c_{Wc3} \cdot W_{c3} + \dot{Z}_{11}$ $c_{Wc3} = c_{Wt}$

3. RESULTS

3.1 Energy and exergy analysis

A 50-piece discretized model was applied to the main heat exchanger T-Q profile, coupling the Unisim and EES power plant code thermodynamic properties packages; the results depend on the CO₂ content of the mixture and are shown in Figures 4 and 5 respectively for R245fa and R1233zd(E) ORC working fluids.

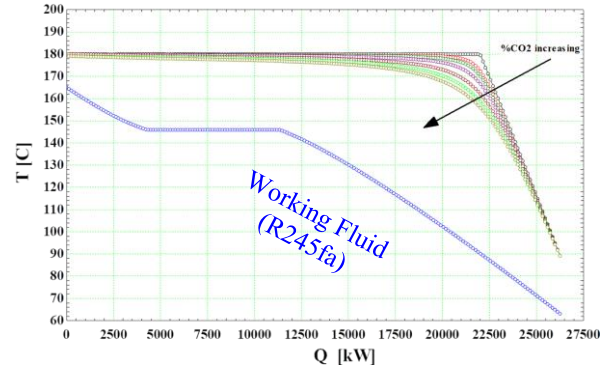


Figure 4: Main heat exchanger T-Q profile (R245fa)

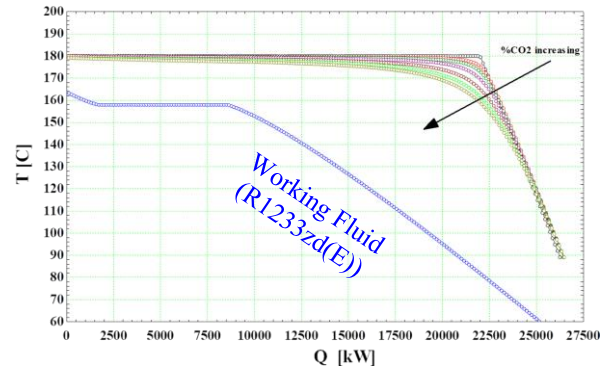


Figure 5: Main heat exchanger T-Q profile (R1233zd(E))

Figure 6 shows the calculated T-s diagram for the CO₂ compression train process.

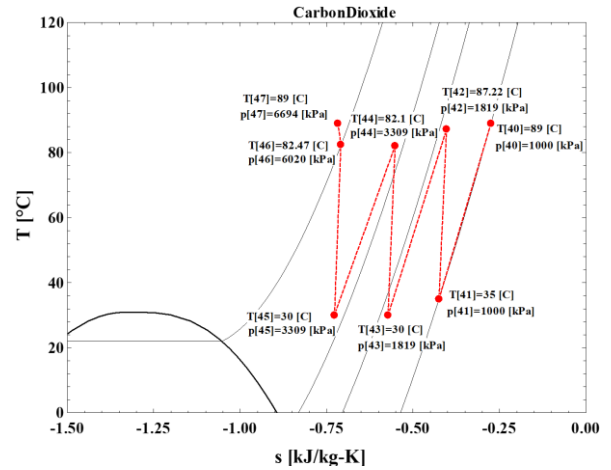


Figure 6: T-s diagram of the CO₂ compression process

Table 3 summarizes the results of the thermodynamic analysis (mass flow rate of the geothermal fluid; energy and exergy efficiency) for the two cases of R245fa and R1233za(E).

Table 3 –Energy and exergy ORC efficiency for various CO₂ content

%CO ₂	R245fa			R1233zd(E)		
	m _{geo} [kg/s]	η	η_x	m _{geo} [kg/s]	η	η_x
0	11.04	0.1861	0.5459	11	0.1867	0.5478
0.5	11.1	0.1861	0.555	11.06	0.1867	0.5568
1	11.15	0.1861	0.5552	11.12	0.1867	0.5571
2	11.27	0.186	0.5573	11.23	0.1866	0.5592
4	11.5	0.1859	0.5609	11.46	0.1866	0.5627
6	11.74	0.1859	0.5642	11.7	0.1865	0.566
8	12	0.1858	0.5672	11.96	0.1864	0.5691

3.2 Exergo-economic analysis

The exergo-economic analysis was applied to the whole equipment data. The cost of the wells drilling was considered indirectly, assuming a cost of the geothermal fluid (point 30 of figure 3) equal to 0.0421 €/kWh (this value was determined in a previous study, Fiaschi et al., 2017). This allowed the evaluation of the investment cost of the whole system, as well as the cost of the electricity produced by the ORC. These results are summarized in Table 4.

Table 4 – Investment cost and cost of electricity

%CO ₂	R245fa		R1233zd(E)	
	€/kW	c€/kWh	€/kW	c€/kWh
0	4288	14.25	3989	13.79
0.5	4288	14.13	3989	13.67
1	4288	14.13	3988	13.66
2	4287	14.1	3988	13.63
4	4286	14.04	3987	13.58
6	4285	13.99	3986	13.53
8	4284	13.95	3985	13.49

3. CONCLUSIONS

The first stage evaluation of an innovative ORC power plant (Castelnuovo Val di Cecina) including complete NCG reinjection was carried out. The model includes the treatment of the geothermal fluid as a mixture of H₂O and 8% CO₂, and the exergy and exergo-economic analyses leading to the evaluation of energy and exergy efficiencies as well as of the production cost of electricity. Geothermal fluid properties (H₂O + CO₂) were calculated through a Unisim 3-rd EOS model; an

EES model of the ORC was run on working fluids R245fa and R1233zd(E), which represent two modern alternatives. The energy efficiency of the power cycle is about 0,185 and is not affected by the CO₂ content of the resource; the exergy efficiency is about 55% and increases with increasing CO₂ content into the geothermal fluid. A production cost of electricity between 13 and 15 c€/kWh was calculated, not including the detailed cost of the well but simply taking into account a lumped cost of the geothermal resource at the current stage of the analysis. No substantial differences between the two working fluids emerged, which favours the choice of R1233zd(E) because of its lower GWP.

ACKNOWLEDGMENTS

The present work is one of the first results within the GECO H2020 Energy European Project, participant University of Florence. Project Partners Graziella GreenPower, IFPEN and Storengy are gratefully acknowledged for providing the Castelnuovo Val di Cecina operating data, and many fruitful discussions.

REFERENCES

- Afgan, N.H. and Carvalho, M.G.: Sustainability assessment of energy systems: An overview of current status. Geothermal energy for developing countries. Balkema, Leiden, The Netherlands, 2002, pp.1-35.
- Arnorsson, S., Sigurdsson, S. and Svavarsson, H., 1982. The chemistry of geothermal waters in Iceland. I. Calculations of aqueous speciation from 0°C to 370 °C. *Geochim. Cosmochim. Acta*, 46,1513-1532.
- Bejan, A., Moran, M., Tsatsaronis, G. *Thermal Design and Optimization*, Wiley, 1995.
- Bertani, R., Thain I., Geothermal power generating plant CO₂ emission survey, *IGA News* 49 (2002) 1-3
- CARBFIX project web site, <https://www.carbfix.com/> (Accessed March 9th, 2019)
- Chiodini, G. and Cioni, R., 1989. Gas geobarometry for hydrothermal systems and its application to some Italian geothermal areas. *Appl. Geochem., Res.*, 4,465-472.
- ContactEnergy, Wairakei-Tauhara Geothermal System Draft System Management Plan. Tahaara II Geothermal Development Project, ContactEnergy, 2010. Available from: <https://contact.co.nz/Assets/pdfs/corporate/environmental/R3DraftSystemManagementPlan.pdf>.
- Di Pippo, R., *Geothermal Power Plants*, Butterworths, 2007
- Duan Z., Sun R., An improved model calculating CO₂ solubility in pure water and aqueous NaCl solutions from 273 to 533 K and from 0 to 2000 bar, *Chemical Geology*, 193, 2003, 257 – 271

- Eylem K., Victor C., Warren. CO₂ -water mixture reinjection into two-phase liquid dominated geothermal reservoirs. *Renewable Energy* 126 (2018), pp. 652-667.
- D. Fiaschi, G. Manfrida, E. Rogai, L. Talluri (2017), *Exergoeconomic analysis and comparison between ORC and Kalina cycles to exploit low and medium-high temperature heat from two different geothermal sites*, *Energy Conversion and Management*, Volume 154, 2017, Pages 503-516, ISSN 0196-8904.
- Kasameyer, R.: Brief guidelines for the development of inputs to CCTS from the technology working group. Working draft, Lawrence Livermore Laboratory, Livermore, CA, 1997.
- Ingimundarson, A, Arnarson, M., Sighvatsson, H., Gunnarsson, T., Design of H₂S Absorption Column at the Hellisheidi Powerplant. Proceedings, World Geothermal Congress, Melbourne, AU, 2015.
- Kaya, E., Zarrouk, S., J., Reinjection of greenhouse gases into geothermal reservoirs, *Int. J., Greenh. Gas Contr.* 67 (2017) 111-129 <https://doi.org/10.1016/j.ijggc.2017.10.015>.
- Kohl, A.L., Nielsen, R., 1997. *Gas Purification*, fifth ed. Gulf Professional Publishing, Houston.
- Kotas, T, *The Exergy Method of Thermal Plants Analysis*, Butterworths, 1985.
- Mahon, W.A.J., McDowel, G.D., Finlayson, J.B., 1980b. Carbon dioxide: its role in geothermal systems. *N.Z.J.Sci.*,23,133-148.
- Manfrida, G., Fiaschi, D., Tempesti, D., Bruscoli, L., improving the environmental sustainability of flash geothermal power plants—a case study, *Sustainability*, 7:15262-15283, 2015
- Nellis, F.A. Klein, F.G. *Mastering EES*, <http://fchart.com/ees/mastering-ees.php>
- Szargut, J., Morris, D.R., and Steward, F.R. *Exergy analysis of thermal, chemical, and metallurgical processes.*, Hemisphere, 1988..
- Turton, R., et al., *Analysis, synthesis and design of chemical processes*, Prentice-Hall, 2009.
- UniSim® Design Simulation Basis, Honeywell International, 2018
- Vaccaro, M., Batini, F., Stolzuoli, M., Bianchi, S., Pizzoli, R., Lisi, S., 2016. Geothermal ORC plant case study in Italy: Castelnuovo Val di Cecina pilot project -design and technical features. Proceedings of the European Geothermal Congress.